Atherosclerosis Susceptibility Loci Identified in an Extremely Atherosclerosis-Resistant Mouse Strain

Jessica S. Rowlan, BA;* Qiongzhen Li, PhD;* Ani Manichaikul, PhD; Qian Wang, MS; Alan H. Matsumoto, MD; Weibin Shi, MD, PhD

Background**—**C3H/HeJ (C3H) mice are extremely resistant to atherosclerosis, especially males. To understand the underlying genetic basis, we performed quantitative trait locus (QTL) analysis on a male F_2 (the second generation from an intercross between 2 inbred strains) cohort derived from an intercross between C3H and C57BL/6 (B6) apolipoprotein E–deficient (*Apoe*$^{-/-}$) mice.

Methods and Results**—**Two hundred forty-six male F_2 mice were started on a Western diet at 8 weeks of age and kept on the diet for 5 weeks. Atherosclerotic lesions in the aortic root and fasting plasma lipid levels were measured. One hundred thirty-four microsatellite markers across the entire genome were genotyped. Four significant QTLs on chromosomes (Chr) 2, 4, 9, and 15 and 4 suggestive loci on Chr1, Chr4, and Chr7 were identified for atherosclerotic lesions. Unexpectedly, the C3H allele was associated with increased lesion formation for 2 of the 4 significant QTLs. Six loci for high-density lipoprotein (HDL), 6 for non-HDL cholesterol, and 3 for triglycerides were also identified. The QTL for atherosclerosis on Chr9 replicated *Ath29*, originally mapped in a female F_2 cohort derived from B6 and C3H *Apoe*$^{-/-}$ mice. This locus coincided with a QTL for HDL, and there was a moderate, but statistically significant, correlation between atherosclerotic lesion sizes and plasma HDL cholesterol levels in F_2 mice.

Conclusions**—**These data indicate that most atherosclerosis susceptibility loci are distinct from those for plasma lipids except for the Chr9 locus, which exerts effect through interactions with HDL. **(*J Am Heart Assoc.* 2013;2:e000260 doi: 10.1161/JAHA.113.000260)**

Key Words: atherosclerosis • cholesterol • mapping • quantitative trait loci • sex

Atherosclerosis is a complex inflammatory disease of large and medium-sized arteries, resulting from interactions between genetic and environmental factors.[1] The mouse is the leading mammalian model organism for finding genes involved in atherosclerosis and many other complex diseases.[2] A number of candidate genes suspected of contributing to the development of atherosclerosis have been tested through construction and analysis of gene knockout or transgenic mice.[3] Inbred mouse strains that display phenotypic differences in atherosclerosis or related traits have been used to conduct quantitative trait locus (QTL) analysis for finding new genes and pathways that give rise to the traits. To date, >18 mouse crosses from 12 inbred strains have been constructed to identify loci for atherosclerosis, leading to the identification of 43 QTLs for aortic plaques (http://www.informatics.jax.org/searches/allele_form.shtml). C3H/HeJ (C3H) and C57BL/6 (B6) are the most phenotypically divergent inbred mouse strains in terms of variation in atherosclerotic lesion sizes in the aortic root.[4] C3H mice develop much smaller lesions than B6 mice when fed an atherogenic diet or deficient in apolipoprotein E (*Apoe*$^{-/-}$),[5,6] In a female F_2 cohort derived from B6.*Apoe*$^{-/-}$ and C3H.*Apoe*$^{-/-}$ mice, we identified a major locus on chromosome (Chr) 9, named *Ath29* (initially named *Ath22*), that had a major effect on atherosclerotic lesion formation in the aortic root.[7] This locus was subsequently replicated in 2 separate intercrosses that developed fatty streak or advanced lesions.[8]

Previous studies have shown that atherosclerosis susceptibility loci mapped from a female population are often different from those mapped from a male population even though they were derived from the same cross.[9–13] In this study, we sought to identify QTLs for atherosclerosis in a male F_2 cohort generated from B6.*Apoe*$^{-/-}$ and C3H.*Apoe*$^{-/-}$ mice. Male mice are more resistant to atherosclerosis than their female counterparts, partially due to higher HDL

From the Departments of Radiology and Medical Imaging (JSR, QL, QW, AHM, WS), Biochemistry & Molecular Genetics (WS), and Public Health Sciences (AM), University of Virginia, Charlottesville, VA.

*Drs Rowlan and Li have contributed equally to this article.

Correspondence to: Weibin Shi, University of Virginia, Box 801339, Snyder 266, 480 Ray C Hunt Drive, Charlottesville, VA 22908. E-mail: ws4v@virginia.edu

Received April 15, 2013; accepted July 17, 2013.

cholesterol levels.[14–16] Thus, the potential genetic link of atherosclerosis with plasma lipids was also explored through the cohort.

Materials and Methods

Mice

B6.*Apoe*$^{-/-}$ mice were purchased from the Jackson Laboratories, and C3H.*Apoe*$^{-/-}$ mice were created in our laboratory. The creation of a male F_2 population from the 2 *Apoe*$^{-/-}$ mouse strains was done as recently reported.[17] Briefly, B6.*Apoe*$^{-/-}$ mice were mated with C3H.*Apoe*$^{-/-}$ mice to generate F_1s, which were intercrossed by brother–sister mating to generate 246 male F_2s. Mice were weaned onto a chow diet at 3 weeks of age. At 8 weeks of age, mice were switched onto a Western diet containing 21% fat, 34.1% sucrose, 0.15% cholesterol, and 19.5% casein (TD 88137; Harlan Laboratories) and maintained on the diet for 5 weeks. Mice were fasted overnight before being killed, and blood was collected via retro-orbital venous plexus puncture with the animals under isoflurane anesthesia. After being bled, mice were killed to allow collection of the heart and tail samples. All procedures were carried out in accordance with the National Institutes of Health guidelines and approved by the institutional Animal Care and Use Committee.

Aortic Lesion Analysis

Atherosclerotic lesions in aortic root were measured as previously reported.[7] Briefly, mice were killed via cervical dislocation after isoflurane anesthesia. The vasculature of the animals was perfusion-fixed with 10% formalin through the left ventricle of the heart. The aortic root and adjacent heart were excised en bloc and embedded in optimal cutting temperature compound. Serial 10-μm-thick cryosections from the middle portion of the ventricle to the aortic arch were collected and mounted on slides. In the region from the appearance to the disappearance of the aortic valves, every other section was collected. In all other regions, every fifth section was collected. Sections were stained with oil red O and hematoxylin and counterstained with fast green. Atherosclerotic lesion areas were measured using an ocular lens with a square-micrometer grid on a light microscope. The lesion areas on all sections were summed and then normalized to 44 sections for each mouse, and this number was used for statistical analysis.

Plasma Lipid Analysis

The measurements of total cholesterol, HDL cholesterol, and triglycerides were performed as reported previously.[18] Briefly, 6 μL of plasma samples (for total cholesterol measurements, plasma was diluted 1:5 in distilled water), lipid standards, and controls was loaded onto a 96-well plate in duplicate and then mixed with 150 μL of cholesterol or triglyceride reagents. After an 8-minute incubation at 37°C, the absorbance at 500 nm was read on a Molecular Devices plate reader. Non-HDL cholesterol was calculated as the difference between total and HDL cholesterol.

Genotyping

DNA was isolated from the tails of mice by using the standard phenol–chloroform extraction and ethanol precipitation method. One hundred thirty-four microsatellite markers on all 19 autosomes and the X chromosome at an interval of approximately 11 cM were screened for all of the F_2 progeny individually by polymerase chain reaction. Parental and F_1 DNA was also typed as controls for each marker so as to readily identify the parental origin of alleles at the marker in F_2s.

Statistical Analysis

QTL analysis was performed using J/qtl for atherosclerotic lesion size and plasma lipid levels in 246 male F_2s that were genotyped for 134 micosatellite markers across the entire genome (the data have been deposited in the Mouse Genome Informatics database), as we previously reported.[7,17,19] J/qtl is a Java graphic user interface for the popular QTL data analysis software R/qtl (http://churchill.jax.org/software/jqtl.shtml). One thousand permutations of trait values were run to define the genomewide logarithm of odds (LOD) score thresholds for significant and suggestive linkage to each trait. Loci that exceeded the 95th percentile of the permutation distribution were defined as significant ($P<0.05$), and those exceeding the 37th percentile were suggestive ($P<0.63$), as recommended by the Complex Trait Consortium.[20] Permutation tests are the standard statistical approach for obtaining threshold values that are adjusted for multiple testing.[21] In these permutation tests, genome scans are repeatedly carried out on shuffled versions of the data to estimate an LOD threshold that is appropriate for the given data set.

ANOVA was performed to determine the statistical significance of differences in phenotypic values of F_2 mice among different genotypes at a specific marker. The mode of inheritance for a QTL was determined based on relative trait values of F_2 mice among 3 different genotypes at the nearest marker: if a heterozygous allele (*BC*) produced the same phenotypic effect as a homozygous allele (*BB* or *CC*), the QTL effect was called “dominant” and the allele with a larger effect was called the “high allele”; if a heterozygous allele produced a phenotypic effect somewhere between the effect of the 2 homozygous alleles (*BB* and *CC*), it was called "additive"; if an allele only expressed a phenotypic effect in the homozygous condition, it was called "recessive"; and if a heterozygous allele produced a phenotypic effect that exceeded the effect of the 2 homozygous alleles, it was called "heterosis."

Prioritization of Positional Candidate Genes

The Sanger SNP database (http://www.sanger.ac.uk/cgi-bin/modelorgs/mousegenomes/snps.pl) was used to prioritize candidate genes for significant atherosclerosis QTLs that had been mapped in ≥2 crosses generated from different parental strains. Probable candidate genes were defined as those with ≥1 single nucleotide polymorphisms (SNPs) in coding or upstream promoter regions that were shared by the parental strains carrying the "high" allele but were different from the parental strains carrying the "low" allele at a QTL.

Results

Trait Value Frequency Distributions

Values of atherosclerotic lesion sizes in the aortic root of 246 male F_2 mice were distributed in a Pareto manner: the number of F_2 mice with a lesion size of ≤10 000 μm^2 is the largest and then decreases as lesion sizes increase (Figure 1). After being transformed using natural logs (LN), the values of atherosclerotic lesion sizes approach a normal distribution. The values of log-transformed HDL cholesterol, non-HDL cholesterol, and log-transformed triglyceride concentrations in F_2 mice are approximately normally distributed. These data were then analyzed using J/qtl software to detect significant and suggestive QTLs affecting the traits.

Atherosclerotic Lesions

We first performed a genomewide scan using untransformed atherosclerotic lesion size data to detect main-effect loci with the nonparametric mode and found 4 significant QTLs, located on

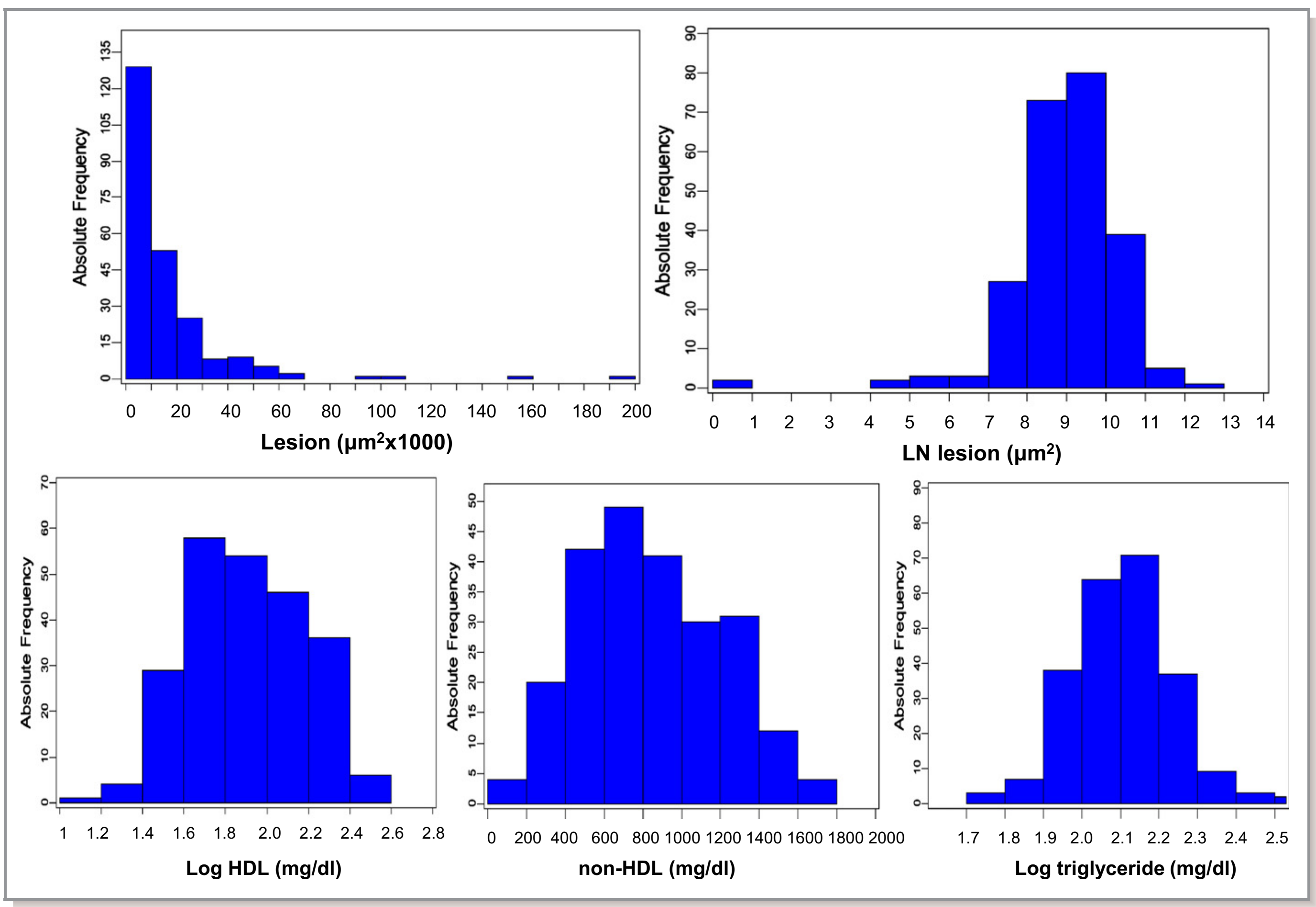

Figure 1. Frequency distributions of atherosclerotic lesion sizes and plasma lipid levels in 246 male F_2 mice after being fed a Western diet for 5 weeks. The F_2 progeny was generated from an intercross between B6.*Apoe*$^{-/-}$ and C3H.*Apoe*$^{-/-}$ mice. Note that the unit for untransformed atherosclerotic lesion sizes is "$\mu m^2 \times 1000$," whereas the unit for LN-transformed atherosclerotic lesion sizes is "μm^2." LN indicates natural logs.

Chr2, Chr4, Chr9, and Chr15, and 2 suggestive QTLs, with 1 on distal Chr4 and 1 on Chr7 (Figure 2). Details of the QTLs found, including locus name, LOD score, peak location, 95% CI, genomewide significance *P* value, high allele, and mode of inheritance, are presented in Table 1. Unexpectedly, the C3H allele was associated with increased lesion sizes for 2 of the 4 significant QTLs, including the Chr2 and Chr15 QTLs (Table 2). The Chr2 locus peaked at 100.5 cM and had a significant LOD score of 3.59 and a genomewide *P* value of 0.041. This locus was overlapping in the CI with *Ath28*, mapped in an Akr.*Apoe*$^{-/-}$×DBA.*Apoe*$^{-/-}$ intercross.[9] The Chr15 locus peaked at 37.8 cM and had a highly significant LOD score of 5.92. This QTL replicated *Ath33*, a locus identified in a B6.*Apoe*$^{-/-}$×C3H.*Apoe*$^{-/-}$ intercross fed a Western diet.[13] The interval mapping plot for Chr4 revealed 2 distinct peaks, each with an LOD score exceeding the suggestive LOD score threshold of 2.05 (Figure 3). The proximal peak occurred at 31.6 cM with a significant LOD score of 3.81, and the distal peak appeared at 77.6 cM with a suggestive LOD score of 2.14. The proximal QTL was partially overlapping with *Ath8*, a suggestive locus mapped in an SM/J×NZB/BINJ intercross,[22] and the distal QTL replicated *Athsq1*, a locus identified in an MOLF/Ei×B6. *Ldlr*$^{-/-}$ backcross.[11] Both loci exhibited a dominant effect from the B6 allele on lesion formation. The Chr9 QTL had a highly significant LOD score of 5.40 and a genomewide *P* value of <0.0001. This QTL replicated *Ath29*, originally identified in a female cohort derived from B6.*Apoe*$^{-/-}$ and C3H.*Apoe*$^{-/-}$ mice.[7] The suggestive QTL on Chr7 replicated *Ath31*, identified in a B6.*Apoe*$^{-/-}$×C3H.*Apoe*$^{-/-}$ intercross.[13]

We then localized QTLs using the LN-transformed atherosclerotic lesion size data and identified 2 additional suggestive QTLs on Chr1 (Figure 2). The proximal QTL peaked at 39.2 cM and had a suggestive LOD score of 2.34. This locus replicated *Ath30*, identified in a B6.*Apoe*$^{-/-}$×C3H.*Apoe*$^{-/-}$ intercross.[13] The distal QTL peaked at 78 cM and had a suggestive LOD score of 2.10. This locus replicated *Ath1*, initially detected in recombinant inbred strains derived from B6 and C3H mice and subsequently replicated in several crosses.[13,15,23,24] Both QTLs affected lesion sizes in a dominant manner from the B6 allele (Table 2).

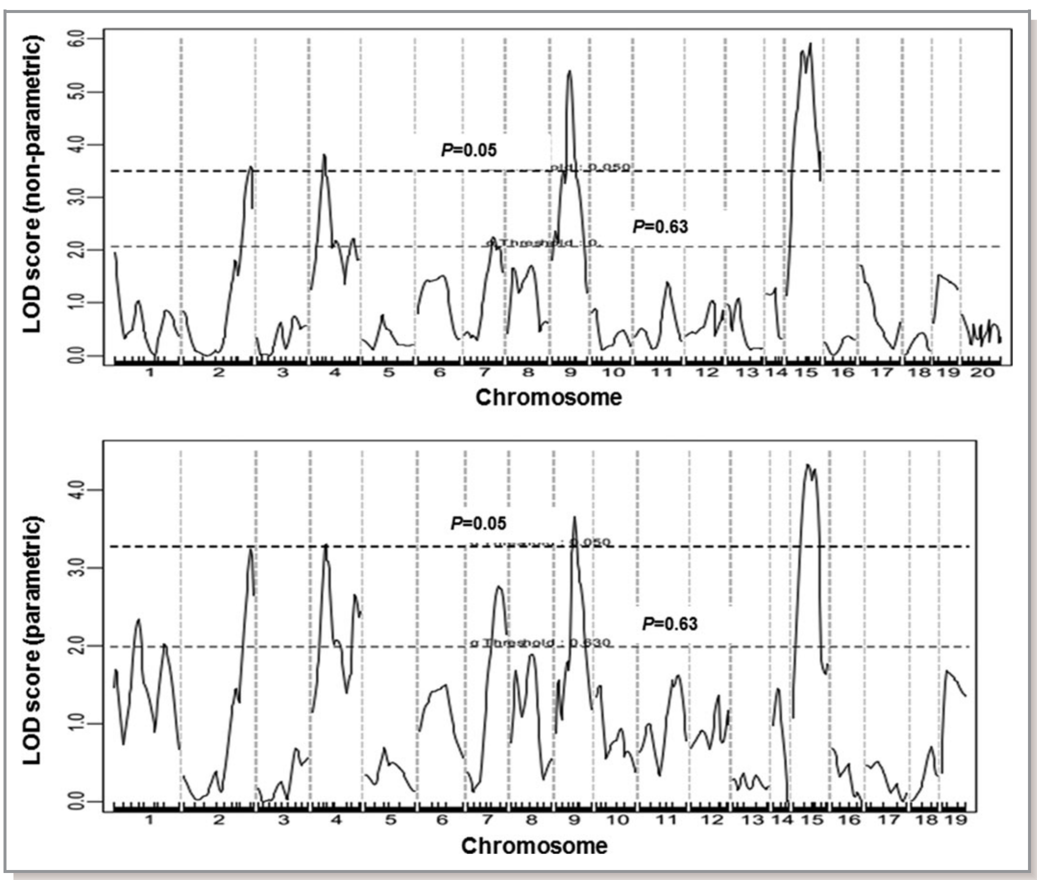

Figure 2. Genomewide QTL analysis to search for loci influencing atherosclerotic lesion sizes in male F_2 mice. Chromosomes 1 through 20 are represented numerically on the *x axis*. The relative width of the space allotted for each chromosome reflects the number of microsatellite markers typed for that chromosome. The *y* axis represents the LOD score. Two horizontal dashed lines denote genomewide thresholds for suggestive (P=0.63) and significant (P=0.05) linkage. The top panel shows a genomewide scan for atherosclerotic lesions using the nonparametric mode, and the bottom panel shows an autosome scan for atherosclerotic lesions using the parametric mode. For the latter scan, the X chromosome was not included due to a strong biased influence from the chromosome. QTL indicates quantitative trait locus; LOD, logarithm of odds.

Table 1. Significant and Suggestive QTLs for Atherosclerosis and Plasma Lipid Levels in Male F_2 Mice Derived from B6.*Apoe*$^{-/-}$ and C3H.*Apoe*$^{-/-}$ Mice

Locus Name	Chr	Trait	LOD*	Peak, cM	95% CI†	*P* Value‡	High Allele§	Mode of Inheritance¶
Ath28	2	Lesion (nonparametric)	**3.59**	100.5	90.2 to 103.8	0.041	C3H	Recessive
Ath8	4	Lesion (nonparametric)	**3.81**	31.6	23.6 to 77.6	0.022	B6	Dominant
Athsq1	4	Lesion (nonparametric)	2.14	77.6	63 to 82.6	…	B6	Dominant
Ath31	7	Lesion (nonparametric)	2.25	59.1	47.1 to 73.0	0.489	B6	Dominant
Ath29	9	Lesion (nonparametric)	**5.40**	44.2	40.2 to 48.2	0.0001	B6	Additive
Ath33	15	Lesion (nonparametric)	**5.92**	37.8	21.8 to 43.8	0.0001	C3H	Additive
Ath30	1	Lesion (parametric)	2.34	39.2	3.7 to 91.7	0.385	B6	Dominant
Ath1	1	Lesion (parametric)	2.10	78	66 to 93	…	B6	Dominant
Ath28	2	Lesion (parametric)	3.24	100.5	88.2 to 103.8	0.054	C3H	Recessive
Ath8	4	Lesion (parametric)	**3.30**	33.6	25.6 to 82.6	0.047	B6	Heterosis
Athsq1	4	Lesion (parametric)	2.65	75.6	67.6 to 82.6	…	B6	Dominant
Ath31	7	Lesion (parametric)	2.77	61.1	51.1 to 73.0	0.175	B6	Dominant
Ath29	9	Lesion (parametric)	**3.65**	46.2	40.2 to 58.2	0.019	B6	Additive
Ath33	15	Lesion (parametric)	**4.33**	25.8	15.2 to 39.8	0.005	C3H	Additive
Hdlq5	1	HDL	**7.30**	67.71	65.67 to 73.67	0.0001	C3H	Additive
Hdlq16	8	HDL	2.11	17.7	13.7 to 45.7	0.617		Heterosis
Hdlq17	9	HDL	3.04	20.2	0 to 34	…	C3H	Additive
Hdlq54	9	HDL	**3.55**	43.91	18.24 to 48.24	0.054	C3H	Additive
Hdlq18	12	HDL	2.81	12.04	10.04 to 44.04	0.228	C3H	Heterosis
Lipq2	13	HDL	3.05	64.72	21.99 to 64.72	0.145	C3H	Dominant
Cq1	1	Non-HDL	**4.92**	75.67	67.71 to 85.67	0.002	C3H	Additive
Chol8	4	Non-HDL	2.51	13.55	13.55 to 57.55	0.323	B6	Additive
Nhdlq12	12	Non-HDL	**6.59**	54.04	30.04 to 58.04	0.0001	B6	Dominant
Chldq8	14	Non-HDL	2.24	29.37	19.37 to 35.37	0.488	C3H	Additive
Nhdlq9	15	Non-HDL	2.43	51.82	3.82 to 53.94	0.367	C3H	Recessive
Nhdlq2	X	Non-HDL	2.22	24.59	20.59 to 58.59	0.511		
Tglq1	1	Triglyceride	**6.42**	77.67	73.67 to 85.67	0.0001	C3H	Additive
Tgq10	2	Triglyceride	2.62	49.35	24.23 to 58.23	0.305	C3H	Dominant
Tgq28	16	Triglyceride	2.51	9.66	9.66 to 35.66	0.355	B6	Dominant

QTL indicates quantitative trait locus; Chr, chromosome; LOD, logarithm of odds.

*LOD scores were obtained from genomewide QTL analysis using J/qtl software. The significant LOD scores are highlighted in bold. The suggestive and significant LOD score thresholds were determined by 1000 permutation tests for each trait. Suggestive and significant LOD scores were 2.045 and 3.362 for atherosclerotic lesion size (nonparametric), 1.986 and 3.277 for natural log–transformed lesion sizes (parametric), 2.123 and 3.559 for HDL cholesterol, 2.087 and 3.49 for non-HDL cholesterol, and 2.12 and 3.432 for triglycerides, respectively.

†The 95% CI in cM defined by a whole genome QTL scan.

‡The *P* values reported represent the level of genomewide significance as they were generated by J/qtl basedon genomewide permutation tests.

§High allele—the allele with a larger allelic effect at the peak marker of a QTL.

¶Mode of inheritance was defined according to allelic effect at the nearest marker of a QTL: dominant, a heterozygous allele produced the same phenotypic effect as a homozygous allele; additive, a heterozygous allele produced a phenotypic effect between the effect of the 2 homozygous alleles; recessive, an allele only expressed a phenotypic effect in the homozygous condition; and heterosis, a heterozygous allele produced a phenotypic effect exceeding the effect of the 2 homozygous alleles.

Plasma Lipid Levels

Genomewide scans revealed that plasma HDL, non-HDL cholesterol, and triglyceride levels were each controlled by multiple QTLs (Figure 4, Table 1). For HDL, 2 significant QTLs, located on Chr1 and Chr9, and 4 suggestive QTLs, located on Chr8, Chr9, Chr12, and Chr13, were identified. The significant QTL on Chr1 replicated *Hdlq5,* which had been mapped in numerous crosses.[25] The interval mapping graph for Chr9 showed 2 distinct QTLs with each surpassing the suggestive LOD score threshold of 2.087 (Figure 5). The distal locus peaked at 43.9 cM and had a significant LOD score of 3.55.

Table 2. Effects of B6 (B) and C3H (C) Alleles in Different QTLs on Atherosclerosis and Plasma Lipids in the Intercross Between B6.*Apoe*$^{-/-}$ and C3H.*Apoe*$^{-/-}$ Mouse Strains

Locus Name[a]	Chr	Trait	LOD	Peak, cM	Closest Marker	BB	BC	CC	*P* Value
Ath28	2	Lesion (nonparametric)	**3.59**	100.5	D2Mit148	12 595±12 897 (n=73)	10 848±10 165 (n=99)	28 271±36 479 (n=56)	1.8E−06
Ath8	4	Lesion (nonparametric)	**3.81**	31.6	D4Mit139	15 296±13 347 (n=59)	16 945±22 166 (n=104)	12 520±24 876 (n=73)	0.396
Athsq1	4	Lesion (nonparametric)	2.14	77.6	D4Mit33	15 861±24 952 (n=53)	17 479±23 433 (n=118)	10 616±12 244 (n=59)	0.136
Ath31	7	Lesion (nonparametric)	2.25	59.1	D7Mit330	17 873±27 165 (n=56)	16 152±20 439 (n=118)	11 153±16 419 (n=60)	0.198
Ath29	9	Lesion (nonparametric)	**5.40**	44.2	D9Mit236	22 162±22 430 (n=54)	15 020±20 472 (n=120)	10 123±20 992 (n=63)	9.26E−03
Ath33	15	Lesion (nonparametric)	**5.92**	37.8	D15Mit188	9386±11 194 (n=48)	14 341±23 011 (n=120)	24 495±25 337 (n=50)	1.95E−03
Ath30	1	Lesion (parametric)	2.34	39.2	D1MIT161	16 369±17 243 (n=53)	16 027±22 747 (n=121)	13 748±22 869 (n=58)	0.765
Ath1	1	Lesion (parametric)	2.1	78	D1Mit270	17 752±24 695 (n=64)	16 318±23 341 (n=102	11 913±14 121 (n=67)	0.261
Ath28	2	Lesion (parametric)	3.24	100.5	D2Mit148	12 595±12 897 (n=74)	10 848±10 165 (n=99)	28 271±36 479 (n=56)	1.8E−06
Ath8	4	Lesion (parametric)	**3.30**	33.6	D4Mit178	14 252±12 034 (n=56)	19 297±28 313 (n=107)	10 376±12 777 (n=69)	2.41E−02
Athsq1	4	Lesion (parametric)	2.65	75.6	D4Mit33	15 861±24 952 (n=53)	17479±23433 (n=118)	10 616±12 244 (n=59)	0.136
Ath31	7	Lesion (parametric)	2.77	61.1	D7Mit330	17 873±27 165 (n=56)	16152±20439 (n=118)	11 153±16 419 (n=60)	0.198
Ath29	9	Lesion (parametric)	**3.65**	46.2	D9Mit236	22 162±22 430 (n=54)	15 020±20 472 (n=120	10 123±20 992 (n=63)	9.26E−03
Ath33	15	Lesion (parametric)	**4.33**	25.8	D15Mit143	9107±10943 (n=47)	14 181±21 364 (n=127)	22 794±25 419 (n=62)	2.41E−03
Hdlq5	1	HDL	**7.30**	67.71	D1Mit425	64.8±45.3 (n=63)	107.1±61.3 (n=113)	114.1±66.7 (n=55)	2.9E−06
Hdlq16	8	HDL	2.11	17.7	D8Mit191	81.0±53.3 (n=56)	107.9±66.8 (n=134)	83.5±49.3 (n=43)	6.5E−03
Hdlq17	9	HDL	3.04	0 to 34	D9Mit297	81.1±53.8 (n=65)	95.0±62.8 (n=105)	116.2±63.8 (n=64)	4.80E−03
Hdlq54	9	HDL	**3.55**	43.91	D9Mit236	73.2±48.7 (n=55)	95.8±60.6 (n=120)	120.2±66.7 (n=61)	1.8E−04
Hdlq18	12	HDL	2.81	12.04	D12Mit84	77.7±52.5 (n=60)	112.3±65.5 (n=98)	92.8±60.6 (n=73)	2.1E−03
Lipq2	13	HDL	3.05	64.72	D13Mit151	73.1±49.1 (n=55)	101.8±60.0 (n=116)	108.4±70.2 (n=64)	3.7E−03
Cq1	1	Non-HDL	**4.92**	75.67	D1Mit270	696.2±341.6 (n=61)	859.7±363.9 (n=101)	976.9±332.6 (n=69)	4.3E−05
Chol8	4	Non-HDL	2.51	13.55	D4Mit192	938.6±353.6 (n=48)	873.3±361.4 (n=106)	730.4±344.9 (n=75)	3.1E−03
Nhdlq12	12	Non-HDL	**6.59**	54.04	D12mit277	865.6±291.4 (n=49)	909.7±373.4 (n=148)	575.3±265.7 (n=38)	1.1E−06
Chldq8	14	Non-HDL	2.24	29.37	D14MIT155	743.9±336.3 (n=68)	869.0±359.5 (n=109)	941.3±377.4 (n=54)	8.1E−03
Nhdlq9	15	Non-HDL	2.43	51.82	D15Mit161	830.6±327.7 (n=54)	798.9±364.9 (n=123)	977.1±358.8 (n=56)	7.9E−03
Nhdlq2	X	Non-HDL	2.22	24.59	DXMit81	804.2±366.2 (n=110)		875.9±358.2 (n=116)	1.4E−01
Tglq1	1	Triglyceride	**6.42**	77.67	D1Mit270	111.6±26.2 (n=61)	135.5±41.6 (n=102)	148.5±48.0 (n=69)	1.9E−06
Tgq10	2	Triglyceride	2.62	49.35	D2Mit126	117.4±34.5 (n=57)	139.3±46.9 (n=124)	135.7±35.6 (n=53)	4.6E−03
Tgq28	16	Triglyceride	2.51	9.66	D16Mit165	133.5±48.7 (n=68)	140.9±42.7 (n=97)	119.0±31.5 (n=62)	3.7E−03

Data are mean±SD. The units for these measurements are μm^2/section for atherosclerotic lesions and mg/dL for plasma lipid levels. The number in the brackets represents the number of progeny with a specific genotype at a peak marker. ANOVA was used to determine the significance level (*P* value) of differences for a specific phenotype among progeny with different genotypes at a specific marker. The significant LOD scores were highlighted in bold. BB indicates homozygous for B6 alleles at the linked peak marker; CC, homozygous for C3H alleles; BC, heterozygous for B6 and C3H alleles at the peak marker; QTL, quantitative trait locus; Chr, chromosome; LOD, logarithm of odds.

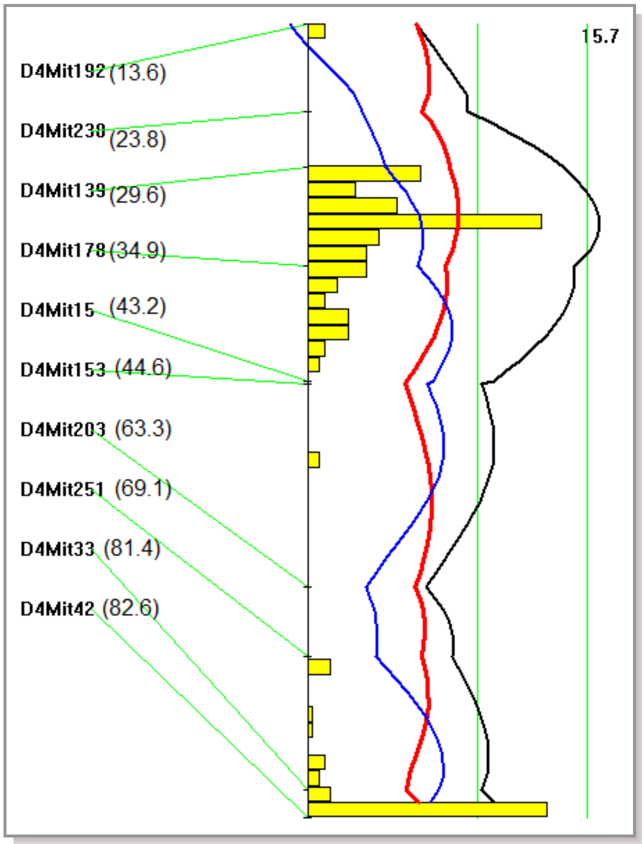

Figure 3. Interval mapping plot for atherosclerotic lesions on chromosome 4. The plot was created with the interval mapping function of Map Manager QTX, which includes a bootstrap test shown as a histogram estimating the CI of a QTL. Two straight vertical lines on the plot represent the genomewide significance thresholds for suggestive and significant linkage. The black line denotes the LOD score calculated at 1-cM intervals. The blue line represents the effect of the B6 allele, and the red line represents the effect of the C3H allele. The histogram indicates the existence of 2 QTLs on the chromosome. The number in the bracket denotes the mapping distance from the centromere of a specific marker in cM. LOD indicates logarithm of odds; QTL, quantitative trait locus.

This QTL coincided precisely with the atherosclerosis susceptibility locus on Chr9. The proximal QTL on Chr9 and the suggestive QTLs on Chr8 and Chr12 corresponded to *Hdlq17, Hdlq16*, and *Hdlq18,* respectively, previously mapped in a B6×129 F_2 population.[26] The QTL on Chr13 was partially overlapping in the confidence interval with *Lipq2*, identified in B6.C-H25C×BALB/cJ F_2 mice.[27] For non-HDL cholesterol, 2 significant QTLs, located on Chr1 and Chr12, and 4 suggestive QTLs, on Chr4, Chr14, Chr15, and ChrX, were identified. The Chr1 QTL replicated *Cq1*, a locus identified in a number of crosses.[28] The Chr12 QTL replicated *Nhdlq12,* previously mapped in female mice derived from an intercross between B6.*Apoe*$^{-/-}$ and C3H.*Apoe*$^{-/-}$ mice.[29] The suggestive QTLs on Chr4, Chr14, Chr15, and ChrX replicated *Chol8*, *Chldq8*, *Nhdlq9*, and *Nhdlq2*, respectively (http://www.informatics.jax.org/phenotypes.shtml). Plasma triglyceride levels were controlled by 1 significant QTL on Chr1 and 2 suggestive QTLs on Chr2 and Chr16, corresponding to *Tglq1*, *Tgq10*, and *Tgq28*, respectively (http://www.informatics.jax.org/phenotypes.shtml).

Relationships Between Plasma Lipids and Atherosclerosis

The associations of atherosclerotic lesion sizes with plasma lipid levels were analyzed using the F_2 population (Figure 6). A significant inverse correlation between lesion sizes and plasma HDL cholesterol levels was observed (r=−0.19, P=0.0041). LN-transformed lesion sizes showed an improved inverse association with plasma HDL cholesterol levels (r=−0.327, P=4.07E−7). F_2 mice with higher HDL cholesterol levels tended to develop smaller atherosclerotic lesions. No significant correlation was observed between non-HDL cholesterol levels and lesion sizes, although there was a trend toward statistical significance between untransformed lesion sizes and non-HDL cholesterol levels (r=0.12, P=0.063).

Prioritization of Positional Candidate Genes for Atherosclerosis QTLs

The C3H allele was responsible for increased lesion formation for 2 of the 4 significant QTLs: *Ath28* on Chr2 and *Ath33* on Chr15. As *Ath28* has been mapped in 2 separate intercrosses, including a previously reported AKR.*Apoe*$^{-/-}$×DBA.*Apoe*$^{-/-}$ cross,[9] we conducted a haplotype analysis using the Sanger SNP database to prioritize positional candidate genes for the QTL. A few candidate genes underneath the linkage peak of *Ath28* were identified, including *Rbm38* (173 Mb), *Cdh4* (179 Mb), *Ss18l1* (179.7 Mb), *Hrh3* (179.8 Mb), *Osbpl2* (179.8 Mb), and *Lama5* (179.9 Mb) (Table 3). These candidates contain ≥1 nonsynonymous SNPs in coding regions or SNPs in the upstream regulatory region that are shared by the low allele strains (B6 and AKR) but are different from the high allele strains (C3H and DBA) at the QTL. These genes were further examined for associations with relevant human diseases using a public accessible genomewide association study database (http://www.genome.gov/GWAStudies/). *Rbm38* has been shown to be associated with variation in the magnitude of statin-mediated reduction in total and LDL cholesterol[30] and *Cdh4* with sudden cardiac arrest in patients with coronary heart disease.[31] *Lama5* was associated with colorectal cancer in European ancestry individuals.[32]

Ath33 on Chr15 has been mapped in 3 independent intercrosses, including 2 B6.*Apoe*$^{-/-}$×C3H.*Apoe*$^{-/-}$ intercrosses and 1 B6.*Apoe*$^{-/-}$×129.*Apoe*$^{-/-}$ intercross.[13,23] C3H and 129 are the high allele strains and B6 is the low allele strain for the QTL. Positional candidate genes, such as

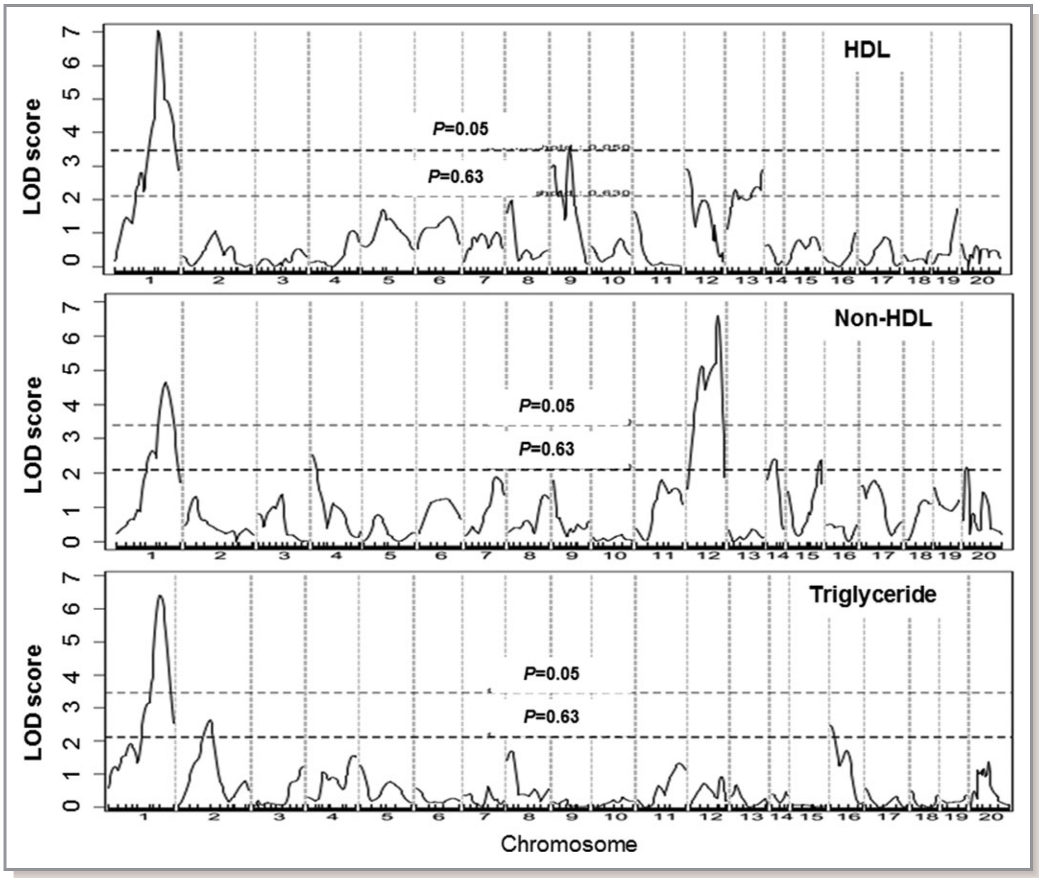

Figure 4. Genomewide scans for HDL, non-HDL cholesterol, and triglyceride levels in the F_2 population. Chromosomes 1 through 20 are represented numerically on the *x axis*, and the *y* axis represents the LOD score. Two horizontal dashed lines denote genomewide thresholds for suggestive and significant linkage. LOD indicates logarithm of odds; HDL, high-density lipoprotein.

Rhpn1 (75.5 Mb), *Apol11b* (77.4 Mb), *Csf2rb2* (78.1 Mb), *Cdc42ep1* (78.6 Mb), *Apobec3* (79.7 Mb), and *Pdgfb* (79.8 Mb), contain ≥1 nonsynonymous SNPs that are shared by the high allele strains but different from the low allele strain. *Cacng2* (77.9 Mb) and *Card10* (78.6 Mb) are positional genes possessing SNPs in the upstream promoter region that are shared by the high allele strains but different from the low allele strain. However, none of these candidate genes have been reported for associations with atherosclerotic arterial disease in recent genomewide association studies.

Discussion

Male mice are more resistant to atherosclerosis than their female counterparts for almost all inbred strains examined.[14,33,34] Higher HDL cholesterol levels have been considered to be a major contributor to the resistance of male mice to atherosclerosis.[14] In this study, we performed QTL analysis using an F_2 cohort from the most phenotypically divergent *Apoe*$^{-/-}$ mouse strains to explore potential genetic connections between atherosclerosis and plasma lipids. Four significant and 4 suggestive QTLs for atherosclerotic lesion sizes and 15 QTLs for plasma HDL, non-HDL cholesterol, and triglyceride levels have been identified. Atherosclerosis susceptibility loci are distinct from those for plasma lipids except for the Chr9 locus, which exerts effects through interactions with HDL.

Ath29 is a significant QTL for atherosclerosis initially identified by our group from a female F_2 cohort derived from B6.*Apoe*$^{-/-}$ and C3H.*Apoe*$^{-/-}$ mice.[7] It is located on mouse Chr9 at 42 cM with the B6 allele contributing to increased lesion sizes. The present study replicated this QTL in a male F_2 population and further revealed its coincidence with an HDL QTL, *Hdlq54*.[32,35] The colocalization of loci for 2 different traits suggests a possibility that these traits are controlled by a same gene. *Elovl5* (77.7 Mb), *Elovl4* (83.7 Mb), and *Me1* (86.5 Mb) are positional candidate genes involved in fatty acid synthesis or elongation, and *Cyb5r4* (86.9 Mb) is a positional candidate gene involved in fatty acid catabolism and oxidative stress.[36] These genes are polymorphic among the parental strains (B6 versus C3H and 129) of 3 intercrosses that have led to detection of the QTL.[23,35] *Tcf12* (71.7 Mb) is also a promising candidate gene with multiple nonsynonymous SNPs between the B6 and C3H strains. It encodes the transcription factor 12 (also called

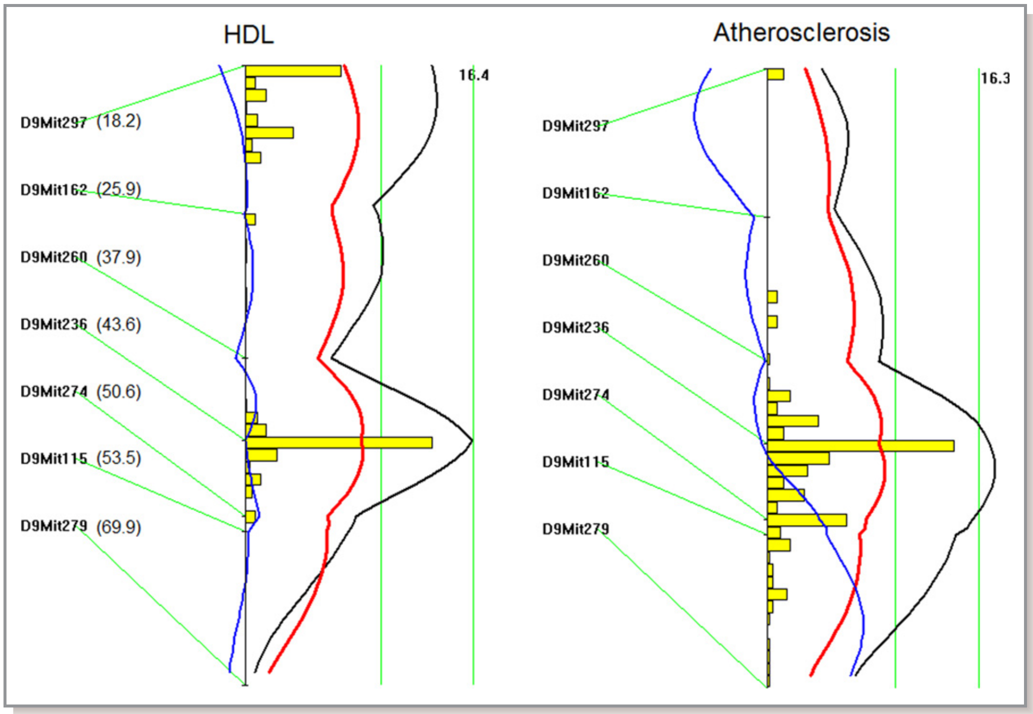

Figure 5. LOD score plots for HDL cholesterol levels (left) and atherosclerotic lesion size (right) on chromosome 9. Plots were created with the interval mapping function of Map Manager QTX. The histogram shown in the plots indicates the confidence interval of a QTL. The distal QTL for HDL coincided with the QTL for atherosclerotic lesions on chromosome 9. The number in the bracket denotes the cM value of a specific marker. LOD indicates logarithm of odds; QTL, quantitative trait locus; HDL, high-density lipoprotein.

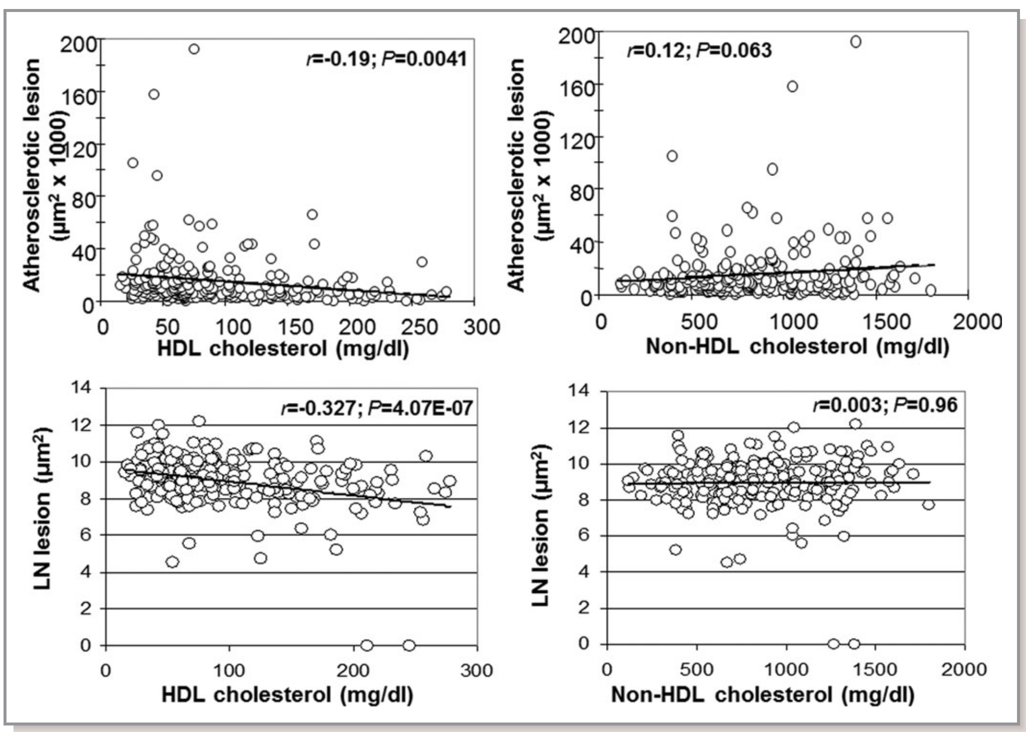

Figure 6. Scatterplots showing relationships of atherosclerotic lesion sizes with HDL and non-HDL cholesterol levels in the F_2 population. Each point represents an individual value of an F_2 mouse. The correlation coefficient (*r*) and significance (*P*) are shown. Plasma levels of HDL but not non-HDL cholesterol were significantly correlated with the sizes of atherosclerotic lesions. Top row: untransformed atherosclerotic lesion sizes in "$\mu m^2 \times 1000$"; bottom row: LN-transformed atherosclerotic lesion sizes in "μm^2". LN indicates natural logs; HDL, high-density lipoprotein.

Table 3. Haplotype Analysis to Prioritize Candidate Genes for Atherosclerosis QTLs on Chromosomes 2 and 15

			Low Allele		High Allele		
Gene	Chromosome	Position	B6	AKR/J	C3H/HeJ	DBA/2J	Consequence
Rbm38	2	172847290	G	G	c	c	5′_UTR
Rbm38	2	172847496	G	G	A	A	5′_UTR
Cdh4	2	179177190	C	C	T	T	5′_UTR
Cdh4	2	179179412	G	G	A	A	NON_SYNONYMOUS_CODING
Ss18l1	2	179777235	C	C	G	G	5′_UTR
Hrh3	2	179835661	C	C	T	T	NON_SYNONYMOUS_CODING
Osbpl2	2	179854116	G	G	A	A	5′_UTR
Lama5	2	179913809	C	C	A	A	NON_SYNONYMOUS_CODING
Lama5	2	179915098	T	T	G	G	NON_SYNONYMOUS_CODING
Lama5	2	179920402	C	C	T	T	NON_SYNONYMOUS_CODING
Lama5	2	179920521	G	G	T	T	NON_SYNONYMOUS_CODING
Lama5	2	179921374	T	T	C	C	NON_SYNONYMOUS_CODING
Lama5	2	179925043	C	C	T	T	NON_SYNONYMOUS_CODING
Lama5	2	179928191	A	A	G	G	5′_UTR
Lama5	2	179928517	G	G	A	A	5′_UTR
Lama5	2	179929976	C	C	T	T	NON_SYNONYMOUS_CODING
Lama5	2	179933048	G	G	A	A	5′_UTR
Lama5	2	179933067	G	G	T	T	NON_SYNONYMOUS_CODING
Lama5	2	179933747	T	T	A	A	5′_UTR
Lama5	2	179933873	G	G	A	A	NON_SYNONYMOUS_CODING
Gene	Chromosome	Position	B6		C3H/HeJ	129	Consequence
Rhpn1	15	75543724	A		G	G	NON_SYNONYMOUS_CODING
Apol11b	15	77468437	A		c	C	NON_SYNONYMOUS_CODING
Cacng2	15	77950358	G		A	A	5′_UTR
Ift27	15	78004380	C		A	A	5′_UTR
Ncf4	15	78075365	T		C	C	5′_UTR
Ncf4	15	78081428	G		A	A	NON_SYNONYMOUS_CODING
Csf2rb2	15	78115054	G		t	t	NON_SYNONYMOUS_CODING
Csf2rb2	15	78115310	T		C	c	NON_SYNONYMOUS_CODING
Csf2rb2	15	78115528	C		t	t	NON_SYNONYMOUS_CODING
Csf2rb2	15	78115654	A		G	G	NON_SYNONYMOUS_CODING
Csf2rb2	15	78115727	T		C	C	NON_SYNONYMOUS_CODING
Csf2rb2	15	78117449	A		G	G	NON_SYNONYMOUS_CODING
Csf2rb2	15	78119364	T		A	A	NON_SYNONYMOUS_CODING
Csf2rb2	15	78122957	C		G	g	NON_SYNONYMOUS_CODING
Csf2rb2	15	78122983	G		a	A	NON_SYNONYMOUS_CODING
Csf2rb2	15	78123018	T		g	G	NON_SYNONYMOUS_CODING
Csf2rb2	15	78123283	G		A	A	NON_SYNONYMOUS_CODING
Csf2rb2	15	78127509	C		G	G	NON_SYNONYMOUS_CODING
Mpst	15	78240804	A		G	G	NON_SYNONYMOUS_CODING

Continued

Table 3. Continued

Gene	Chromosome	Position	B6		C3H/HeJ	129	Consequence
Sstr3	15	78370921	C		T	T	NON_SYNONYMOUS_CODING
Sstr3	15	78370941	G		A	A	NON_SYNONYMOUS_CODING
Sstr3	15	78371011	C		G	G	5′_UTR
Sstr3	15	78374301	G		A	A	5′_UTR
Sstr3	15	78374693	A		G	G	5′_UTR
Sstr3	15	78374764	T		C	C	5′_UTR
Gm6723	15	78384992	C		T	T	NON_SYNONYMOUS_CODING
Gm6723	15	78385151	G		C	C	NON_SYNONYMOUS_CODING
Mfng	15	78603821	A		G	G	5′_UTR
Card10	15	78633071	G		A	A	5′_UTR
Card10	15	78633319	T		C	C	5′_UTR
Cdc42ep1	15	78677764	G		A	A	5′_UTR
Cdc42ep1	15	78679988	T		C	C	NON_SYNONYMOUS_CODING
Cdc42ep1	15	78680104	G		A	A	NON_SYNONYMOUS_CODING
Cdc42ep1	15	78680263	G		A	A	NON_SYNONYMOUS_CODING
Lgals2	15	78681495	T		C	C	NON_SYNONYMOUS_CODING
Gcat	15	78873505	A		G	G	NON_SYNONYMOUS_CODING
Micall1	15	78957630	C		T	T	NON_SYNONYMOUS_CODING
Pick1	15	79060137	A		G	G	5′_UTR
Pick1	15	79079229	A		G	G	NON_SYNONYMOUS_CODING
Pick1	15	79086211	A		C	C	NON_SYNONYMOUS_CODING
Pick1	15	79086466	G		T	T	NON_SYNONYMOUS_CODING
Pick1	15	79086508	A		g	G	NON_SYNONYMOUS_CODING
Pick1	15	79086512	C		g	G	NON_SYNONYMOUS_CODING
Tmem184b	15	79209126	C		A	A	5′_UTR
Csnk1e	15	79269395	A		G	G	5′_UTR
Csnk1e	15	79271799	C		T	T	5′_UTR
Nptxr	15	79624881	T		G	G	NON_SYNONYMOUS_CODING
Apobec3	15	79722929	C		A	A	5′_UTR
Apobec3	15	79725453	A		T	T	5′_UTR
Apobec3	15	79725492	T		A	A	5′_UTR
Apobec3	15	79725494	T		G	G	5′_UTR
Apobec3	15	79725534	A		G	G	5′_UTR
Apobec3	15	79725547	G		A	A	5′_UTR
Apobec3	15	79725550	T		A	A	5′_UTR
Apobec3	15	79725566	G		A	A	5′_UTR
Apobec3	15	79725868	G		A	A	5′_UTR
Apobec3	15	79725887	G		C	C	NON_SYNONYMOUS_CODING
Apobec3	15	79725897	A		T	T	NON_SYNONYMOUS_CODING
Apobec3	15	79725900	G		A	A	NON_SYNONYMOUS_CODING
Apobec3	15	79728257	A		G	G	NON_SYNONYMOUS_CODING

Continued

Table 3. Continued

Gene	Chromosome	Position	B6		C3H/HeJ	129	Consequence
Apobec3	15	79728260	G		C	C	NON_SYNONYMOUS_CODING
Apobec3	15	79728323	G		A	A	NON_SYNONYMOUS_CODING
Apobec3	15	79728327	A		G	G	NON_SYNONYMOUS_CODING
Apobec3	15	79728339	C		A	A	NON_SYNONYMOUS_CODING
Apobec3	15	79728604	G		A	A	NON_SYNONYMOUS_CODING
Apobec3	15	79729463	T		C	C	NON_SYNONYMOUS_CODING
Apobec3	15	79729537	G		C	C	NON_SYNONYMOUS_CODING
Apobec3	15	79735878	A		G	G	NON_SYNONYMOUS_CODING
Apobec3	15	79735881	G		C	C	NON_SYNONYMOUS_CODING
Apobec3	15	79735885	C		T	T	NON_SYNONYMOUS_CODING
Apobec3	15	79735953	C		G	G	NON_SYNONYMOUS_CODING
Apobec3	15	79736838	C		T	T	NON_SYNONYMOUS_CODING
Apobec3	15	79737380	G		A	A	NON_SYNONYMOUS_CODING
Cbx7	15	79749323	C		T	T	NON_SYNONYMOUS_CODING
Cbx7	15	79749453	G		C	C	NON_SYNONYMOUS_CODING
Cbx7	15	79764235	T		G	G	NON_SYNONYMOUS_CODING
Cbx7	15	79764259	A		T	T	STOP_GAINED
Cbx7	15	79764307	A		T	T	NON_SYNONYMOUS_CODING
Cbx7	15	79801396	G		T	T	5′_UTR
Cbx7	15	79801461	A		C	C	5′_UTR
Pdgfb	15	79830813	C		T	T	NON_SYNONYMOUS_CODING
Pdgfb	15	79844499	T		G	G	5′_UTR
Pdgfb	15	79844550	A		C	C	5′_UTR
Pdgfb	15	79844807	G		T	T	5′_UTR
Pdgfb	15	79844895	G		A	A	5′_UTR

Analysis was performed using the Sanger SNP database (http://www.sanger.ac.uk/cgi-bin/modelorgs/mousegenomes/snps.pl). QTL indicates quantitative trait locus.

HTF4 or HEB), a member of the helix-loop-helix protein family.[37] The product of *Tcf12* has diverse functions, including downregulating E-cadherin expression, enhancing cell migration and invasion,[38] and activating T-lymphocyte differentiation,[39] all of which have a role in atherosclerosis.

An interesting finding of this study is the detection of atherosclerosis susceptibility QTLs on Chr2 and Chr15 in which the C3H allele contributed to increased lesion sizes. F_2 mice homozygous for the C3H allele at the loci had larger lesion sizes than those homozygous for the B6 allele. This finding was unexpected given the extremity of resistance that C3H.*Apoe*$^{-/-}$ mice exhibit during the development of atherosclerosis. However, this may not be surprising given the fact that QTL mapping detects loci based on the phenotypic variance among different genotypes at genetic markers within an F_2 or N_2 (second backcross generation) population but not on the phenotypic variance between the 2 parental strains. Both F_2s and N_2s are genetically and phenotypically diverse compared with both parents and thus can lead to revelations of cryptic genetic effects. Atherosclerosis susceptibility loci derived from the resistant strains of crosses have been previously detected in at least 3 independent crosses, including a B6×FVB/N Ldlr$^{-/-}$ intercross, B6×FVB/N *Apoe*$^{-/-}$ intercross, and a B×H *Apoe*$^{-/-}$ intercross.[10,12,13] The Chr2 QTL replicated *Ath28*, originally identified in a DBA/2.*Apoe*$^{-/-}$×AKR.*Apoe*$^{-/-}$ intercross[9] and recently mapped in a B6.*Apoe*$^{-/-}$×129.*Apoe*$^{-/-}$ intercross.[23] The CI of the Chr2 QTL (90 to 104 cM) is corresponding to human Chr20q13, a region associated with sudden cardiac arrest in patients with coronary artery disease and inflammatory and autoimmunal diseases.[31,40,41] The 2 strongest candidate genes for this QTL are *Lama5* and *Cdh4*. *Lama5* encodes laminin, α5, which, together with collagen IV, nidogen/entactin, and heparan sulfate proteoglycans,

Table 4. QTLs for Atherosclerosis and Plasma Lipids Identified in the Present Male Versus the Previously Reported Female F_2 Cohort Derived From B6.*Apoe*$^{-/-}$ and C3H.*Apoe*$^{-/-}$ Mice

Locus Name	Chr	Trait	LOD (Male)	LOD (Female)
Ath30	1	Lesion	2.34	…
Ath1	1	Lesion	2.10	…
Ath28	2	Lesion	**3.59**	…
Ath8	4	Lesion	**3.30**	…
Athsq1	4	Lesion	2.65	…
Ath31	7	Lesion	2.77	…
Ath29	9	Lesion	**3.65**	**4.1**
Ath19	11	Lesion	…	2.4
Ath33	15	Lesion	**4.33**	…
Hdlq5	1	HDL	**7.30**	3.0
Hdlq21	3	HDL	…	2.3
Hdlq16	8	HDL	2.11	…
Hdlq17	9	HDL	3.04	…
Hdlq54	9	HDL	**3.55**	…
Hdlq18	12	HDL	2.81	…
Lipq2	13	HDL	3.05	…
Cq1	1	Non-HDL	**4.92**	**6.3**
Chol8	4	Non-HDL	2.51	…
Chldq3	5	Non-HDL	…	2.2
Nhdlq11	9	Non-HDL	…	2.5
Nhdlq12	12	Non-HDL	**6.59**	…
Chldq8	14	Non-HDL	2.24	…
Nhdlq9	15	Non-HDL	2.43	…
Nhdlq2	X	Non-HDL	2.22	…
Tglq1	1	Triglyceride	**6.42**	**3.8**
Tgq10	2	Triglyceride	2.62	…
Trigg2	8	Triglyceride	…	3.2
Tgq28	16	Triglyceride	2.51	…

QTL indicates quantitative trait locus; Chr, chromosome; LOD, logarithm of odds; male: the present male F_2 cohort derived from B6.*Apoe*$^{-/-}$ and C3H.*Apoe*$^{-/-}$ mice; female: the female F_2 cohort derived from B6.*Apoe*$^{-/-}$ and C3H.*Apoe*$^{-/-}$ mice previously reported by our group.[7] The significant LOD scores were highlighted in bold.

constitutes the structural component of vascular basement membrane.[42] *Cdh4* encodes cadherin 4, a calcium-dependent transmembrane adhesion molecule. The protein products of *Lama5* and *Cdh4* have a broad range of functions, including direct cell–cell cohesion, regulation of cell migration, proliferation, survival, and cell signaling.[43,44]

The Chr15 QTL replicated *Ath33*, previously mapped in a B6.*Apoe*$^{-/-}$×C3H.*Apoe*$^{-/-}$ cross and a B6.*Apoe*$^{-/-}$×129.*Apoe*$^{-/-}$ intercross.[13,23] The CI (22 to 44 cM) of this locus corresponds to human Chr8q24 and Chr22q13, regions that are associated with carotid intima-media thickness,[45] sudden cardiac arrest in patients with coronary heart disease,[31] Crohn disease,[46] and inflammatory bowel disease.[47] The strongest candidate gene for the Chr15 QTL is *Pdgfb*, which encodes the platelet-derived growth factor-β polypeptide. Blood cells, especially monocytes and platelets, are a major source of platelet-derived growth factor-β after being activated.[48] The absence of *Pdgfb* in circulating cells promotes inflammatory responses and early atherosclerosis and delays fibrous cap formation in *Apoe*$^{-/-}$ mice.[49,50]

QTLs on distal Chr1 contributed to major variations in plasma HDL, non-HDL cholesterol, and triglyceride levels of the cross. This finding is consistent with our previous observation in a female cohort derived from an intercross between B6.*Apoe*$^{-/-}$ and C3H.*Apoe*$^{-/-}$ mice.[29] *Apoa2* is a well-characterized QTL gene in the distal Chr1 region accounting for variations in plasma lipid levels of mice.[51] *Soat1* is also a QTL gene in the region that has been confirmed to contribute to variations in plasma levels of lipids, especially HDL cholesterol.[52] A significant QTL for non-HDL cholesterol was mapped to Chr12 at 54 cM in the current cross. This QTL was partially overlapping in the CI with *Nhdlq12*, mapped in a B6.*Apoe*$^{-/-}$×C3H.*Apoe*$^{-/-}$ intercross.[29] One prominent candidate gene for this QTL is *Cyp46a1*, encoding a member of the cytochrome P450 superfamily of monooxygenases that converts cholesterol to 24S-hydroxycholesterol.[53] The oxysterol products activate the liver X receptor NR1H2 and are subsequently metabolized to esters by sterol o-acyltransferase 1.

A moderate but statistically significant reverse correlation was observed between plasma HDL cholesterol levels and atherosclerotic lesion sizes in this cross. This finding supports the concept that HDL is protective against atherosclerosis. However, such a correlation was not observed in female F_2 mice derived from B6.*Apoe*$^{-/-}$ and C3H.*Apoe*$^{-/-}$ mice.[7] The HDL cholesterol levels in the male F_2s were ≈3× higher and exhibited larger variance compared with the female F_2s (96.6±61.7 versus 34.0±27.4 mg/dL), which might explain why statistical associations with atherosclerosis were observed in the males but not in the females. We have also observed a significant reverse correlation between plasma HDL cholesterol levels and atherosclerotic lesion sizes in a B6.*Apoe*$^{-/-}$×BALB/c.*Apoe*$^{-/-}$ intercross, whose HDL levels are higher and display a large variance.[54] No significant correlation between plasma levels of non-HDL cholesterol and sizes of atherosclerotic lesions was observed in this cross or in previous crosses.[7,13,29,54] This finding suggests that in the absence of *Apoe*, other genetic factors than those involved in regulating plasma lipids play a key role in atherosclerosis. In the previous female F_2 cohort derived from B6.*Apoe*$^{-/-}$ and C3H.*Apoe*$^{-/-}$ mice, we only detected 2 QTLs for atherosclerosis and 5 QTLs for plasma lipid levels.[7] In contrast, in the present male F_2 cohort, we have identified 8 QTLs for atherosclerosis and 15 QTLs for plasma lipid levels (Table 4) despite the fact that the 2 intercrosses were derived from the same parental strains. There were several factors that could contribute to the discrepancy in the results between the 2 crosses: first, the previous female F_2 mice were fed a Western diet for 12 weeks starting at 6 weeks of age, while the present male F_2 mice were fed the diet for 5 weeks starting at 8 weeks of age. Thus, female F_2 mice should have developed larger and more advanced lesions than male F_2 mice. Genetic factors could exert effect differently on different stages of atherosclerosis. Second, as discussed earlier, the HDL cholesterol level in the male F_2s was much higher and exhibited larger variance compared with the female F_2s, which was conducive to the identification of QTLs for the trait. Third, the sex of the mice could exert a significant influence on genetic factors on atherosclerosis, as previously illustrated.[9,10,13] Finally, as the 2 crosses were constructed in different time, environmental factors could influence the results.

In summary, we have identified a number of QTLs affecting atherosclerosis and plasma lipid levels using a male F_2 cohort derived from B6.*Apoe*$^{-/-}$ and C3H.*Apoe*$^{-/-}$ mice. Atherosclerosis susceptibility loci are independent of those for plasma lipids except for the Chr9 QTL, which appears to exert effects through interactions with HDL. Through haplotype analysis, we have narrowed the list of candidate genes for major atherosclerosis susceptibility loci.

Sources of funding

This work was supported by National Institutes of Health grant HL82881. The original data of this cross associated with this article have been submitted to the Mouse Genome Informatics database.

Disclosures

None.

References

1. Stylianou IM, Bauer RC, Reilly MP, Rader DJ. Genetic basis of atherosclerosis: insights from mice and humans. *Circ Res*. 2012;110:337–355.
2. Peters LL, Robledo RF, Bult CJ, Churchill GA, Paigen BJ, Svenson KL. The mouse as a model for human biology: a resource guide for complex trait analysis. *Nat Rev Genet*. 2007;8:58–69.
3. Wang X, Ishimori N, Korstanje R, Rollins J, Paigen B. Identifying novel genes for atherosclerosis through mouse-human comparative genetics. *Am J Hum Genet*. 2005;77:1–15.
4. Paigen B, Morrow A, Brandon C, Mitchell D, Holmes P. Variation in susceptibility to atherosclerosis among inbred strains of mice. *Atherosclerosis*. 1985;57:65–73.
5. Paigen B, Morrow A, Holmes PA, Mitchell D, Williams RA. Quantitative assessment of atherosclerotic lesions in mice. *Atherosclerosis*. 1987;68:231–240.
6. Shi W, Wang NJ, Shih DM, Sun VZ, Wang X, Lusis AJ. Determinants of atherosclerosis susceptibility in the C3H and C57BL/6 mouse model: evidence for involvement of endothelial cells but not blood cells or cholesterol metabolism. *Circ Res*. 2000;86:1078–1084.
7. Su Z, Li Y, James JC, McDuffie M, Matsumoto AH, Helm GA, Weber JL, Lusis AJ, Shi W. Quantitative trait locus analysis of atherosclerosis in an intercross between C57BL/6 and C3H mice carrying the mutant apolipoprotein E gene. *Genetics*. 2006;172:1799–1807.
8. Wang SS, Shi W, Wang X, Velky L, Greenlee S, Wang MT, Drake TA, Lusis AJ. Mapping, genetic isolation, and characterization of genetic loci that determine resistance to atherosclerosis in C3H mice. *Arterioscler Thromb Vasc Biol*. 2007;27:2671–2676.
9. Smith JD, Bhasin JM, Baglione J, Settle M, Xu Y, Barnard J. Atherosclerosis susceptibility loci identified from a strain intercross of apolipoprotein E-deficient mice via a high-density genome scan. *Arterioscler Thromb Vasc Biol*. 2006;26:597–603.
10. Teupser D, Tan M, Persky AD, Breslow JL. Atherosclerosis quantitative trait loci are sex- and lineage-dependent in an intercross of C57BL/6 and FVB/N low-density lipoprotein receptor-/- mice. *Proc Natl Acad Sci USA*. 2006;103:123–128.
11. Welch CL, Bretschger S, Latib N, Bezouevski M, Guo Y, Pleskac N, Liang CP, Barlow C, Dansky H, Breslow JL, Tall AR. Localization of atherosclerosis susceptibility loci to chromosomes 4 and 6 using the Ldlr knockout mouse model. *Proc Natl Acad Sci USA*. 2001;98:7946–7951.
12. Dansky HM, Shu P, Donavan M, Montagno J, Nagle DL, Smutko JS, Roy N, Whiteing S, Barrios J, McBride TJ, Smith JD, Duyk G, Breslow JL, Moore KJ. A phenotype-sensitizing Apoe-deficient genetic background reveals novel

atherosclerosis predisposition loci in the mouse. *Genetics*. 2002;160:1599–1608.

13. Wang SS, Schadt EE, Wang H, Wang X, Ingram-Drake L, Shi W, Drake TA, Lusis AJ. Identification of pathways for atherosclerosis in mice: integration of quantitative trait locus analysis and global gene expression data. *Circ Res*. 2007;101:e11–e30.
14. Paigen B, Holmes PA, Mitchell D, Albee D. Comparison of atherosclerotic lesions and HDL-lipid levels in male, female, and testosterone-treated female mice from strains C57BL/6, BALB/c, and C3H. *Atherosclerosis*. 1987;64:215–221.
15. Paigen B, Mitchell D, Reue K, Morrow A, Lusis AJ, LeBoeuf RC. Ath-1, a gene determining atherosclerosis susceptibility and high density lipoprotein levels in mice. *Proc Natl Acad Sci USA*. 1987;84:3763–3767.
16. Qiao JH, Xie PZ, Fishbein MC, Kreuzer J, Drake TA, Demer LL, Lusis AJ. Pathology of atheromatous lesions in inbred and genetically engineered mice. Genetic determination of arterial calcification. *Arterioscler Thromb*. 1994;14:1480–1497.
17. Yuan Z, Pei H, Roberts DJ, Zhang Z, Rowlan JS, Matsumoto AH, Shi W. Quantitative trait locus analysis of neointimal formation in an intercross between C57BL/6 and C3H/HeJ apolipoprotein E-deficient mice. *Circ Cardiovasc Genet*. 2009;2:220–228.
18. Tian J, Pei H, James JC, Li Y, Matsumoto AH, Helm GA, Shi W. Circulating adhesion molecules in apoE-deficient mouse strains with different atherosclerosis susceptibility. *Biochem Biophys Res Commun*. 2005;329:1102–1107.
19. Su Z, Li Y, James JC, Matsumoto AH, Helm GA, Lusis AJ, Shi W. Genetic linkage of hyperglycemia, body weight and serum amyloid-P in an intercross between C57BL/6 and C3H apolipoprotein E-deficient mice. *Hum Mol Genet*. 2006;15:1650–1658.
20. Abiola O, Angel JM, Avner P, Bachmanov AA, Belknap JK, Bennett B, Blankenhorn EP, Blizard DA, Bolivar V, Brockmann GA, Buck KJ, Bureau JF, Casley WL, Chesler EJ, Cheverud JM, Churchill GA, Cook M, Crabbe JC, Crusio WE, Darvasi A, de Haan G, Dermant P, Doerge RW, Elliot RW, Farber CR, Flaherty L, Flint J, Gershenfeld H, Gibson JP, Gu J, Gu W, Himmelbauer H, Hitzemann R, Hsu HC, Hunter K, Iraqi FF, Jansen RC, Johnson TE, Jones BC, Kempermann G, Lammert F, Lu L, Manly KF, Matthews DB, Medrano JF, Mehrabian M, Mittlemann G, Mock BA, Mogil JS, Montagutelli X, Morahan G, Mountz JD, Nagase H, Nowakowski RS, O'Hara BF, Osadchuk AV, Paigen B, Palmer AA, Peirce JL, Pomp D, Rosemann M, Rosen GD, Schalkwyk LC, Seltzer Z, Settle S, Shimomura K, Shou S, Sikela JM, Siracusa LD, Spearow JL, Teuscher C, Threadgill DW, Toth LA, Toye AA, Vadasz C, Van Zant G, Wakeland E, Williams RW, Zhang HG, Zou F, Complex Trait Consortium. The nature and identification of quantitative trait loci: a community's view. *Nat Rev Genet*. 2003;4:911–916.
21. Doerge RW, Churchill GA. Permutation tests for multiple loci affecting a quantitative character. *Genetics*. 1996;142:285–294.
22. Korstanje R, Eriksson P, Samnegard A, Olsson PG, Forsman-Semb K, Sen S, Churchill GA, Rollins J, Harris S, Hamsten A, Paigen B. Locating Ath8, a locus for murine atherosclerosis susceptibility and testing several of its candidate genes in mice and humans. *Atherosclerosis*. 2004;177:443–450.
23. Tomita H, Zhilicheva S, Kim S, Maeda N. Aortic arch curvature and atherosclerosis have overlapping quantitative trait loci in a cross between 129S6/SvEvTac and C57BL/6J apolipoprotein E-null mice. *Circ Res*. 2010;106:1052–1060.
24. Zhang Z, Rowlan JS, Wang Q, Shi W. Genetic analysis of atherosclerosis and glucose homeostasis in an intercross between C57BL/6 and BALB/cJ apolipoprotein E-deficient mice. *Circ Cardiovasc Genet*. 2012;5:190–201.
25. Wang X, Paigen B. Genetics of variation in HDL cholesterol in humans and mice. *Circ Res*. 2005;96:27–42.
26. Ishimori N, Li R, Kelmenson PM, Korstanje R, Walsh KA, Churchill GA, Forsman-Semb K, Paigen B. Quantitative trait loci analysis for plasma HDL-cholesterol concentrations and atherosclerosis susceptibility between inbred mouse strains C57BL/6J and 129S1/SvImJ. *Arterioscler Thromb Vasc Biol*. 2004;24:161–166.
27. Welch CL, Bretschger S, Wen PZ, Mehrabian M, Latib N, Fruchart-Najib J, Fruchart JC, Myrick C, Lusis AJ. Novel QTLs for HDL levels identified in mice by controlling for Apoa2 allelic effects: confirmation of a chromosome 6 locus in a congenic strain. *Physiol Genomics*. 2004;17:48–59.
28. Wang X, Paigen B. Genome-wide search for new genes controlling plasma lipid concentrations in mice and humans. *Curr Opin Lipidol*. 2005;16:127–137.
29. Li Q, Li Y, Zhang Z, Gilbert TR, Matsumoto AH, Dobrin SE, Shi W. Quantitative trait locus analysis of carotid atherosclerosis in an intercross between C57BL/6 and C3H apolipoprotein E-deficient mice. *Stroke*. 2008;39:166–173.
30. Barber MJ, Mangravite LM, Hyde CL, Chasman DI, Smith JD, McCarty CA, Li X, Wilke RA, Rieder MJ, Williams PT, Ridker PM, Chatterjee A, Rotter JI, Nickerson DA, Stephens M, Krauss RM. Genome-wide association of lipid-lowering response to statins in combined study populations. *PLoS ONE*. 2010;5:e9763.
31. Aouizerat BE, Vittinghoff E, Musone SL, Pawlikowska L, Kwok PY, Olgin JE, Tseng ZH. GWAS for discovery and replication of genetic loci associated with sudden cardiac arrest in patients with coronary artery disease. *BMC Cardiovasc Disord*. 2011;11:29.
32. Houlston RS, Cheadle J, Dobbins SE, Tenesa A, Jones AM, Howarth K, Spain SL, Broderick P, Domingo E, Farrington S, Prendergast JG, Pittman AM, Theodoratou E, Smith CG, Olver B, Walther A, Barnetson RA, Churchman M, Jaeger EE, Penegar S, Barclay E, Martin L, Gorman M, Mager R, Johnstone E, Midgley R, Niittymaki I, Tuupanen S, Colley J, Idziaszczyk S, COGENT Consortium, Thomas HJ, Lucassen AM, Evans DG, Maher ER, CORGI Consortium, COIN Collaborative Group, COINB Collaborative Group, Maughan T, Dimas A, Dermitzakis E, Cazier JB, Aaltonen LA, Pharoah P, Kerr DJ, Carvajal-Carmona LG, Campbell H, Dunlop MG, Tomlinson IP. Meta-analysis of three genome-wide association studies identifies susceptibility loci for colorectal cancer at 1q41, 3q26.2, 12q13.13 and 20q13.33. *Nat Genet*. 2010;42:973–977.
33. Smith DD, Tan X, Tawfik O, Milne G, Stechschulte DJ, Dileepan KN. Increased aortic atherosclerotic plaque development in female apolipoprotein E-null mice is associated with elevated thromboxane A2 and decreased prostacyclin production. *J Physiol Pharmacol*. 2010;61:309–316.
34. Teupser D, Persky AD, Breslow JL. Induction of atherosclerosis by low-fat, semisynthetic diets in LDL receptor-deficient C57BL/6J and FVB/NJ mice: comparison of lesions of the aortic root, brachiocephalic artery, and whole aorta (en face measurement). *Arterioscler Thromb Vasc Biol*. 2003;23:1907–1913.
35. Su Z, Wang X, Tsaih SW, Zhang A, Cox A, Sheehan S, Paigen B. Genetic basis of HDL variation in 129/SvImJ and C57BL/6J mice: importance of testing candidate genes in targeted mutant mice. *J Lipid Res*. 2009;50:116–125.
36. Xu M, Wang W, Frontera JR, Neely MC, Lu J, Aires D, Hsu FF, Turk J, Swerdlow RH, Carlson SE, Zhu H. Ncb5or deficiency increases fatty acid catabolism and oxidative stress. *J Biol Chem*. 2011;286:11141–11154.
37. Zhang Y, Babin J, Feldhaus AL, Singh H, Sharp PA, Bina M. HTF4: a new human helix-loop-helix protein. *Nucleic Acids Res*. 1991;19:4555.
38. Chen WS, Chen CC, Chen LL, Lee CC, Huang TS. Secreted heat shock protein 90alpha induces NF-kappaB-mediated TCF12 expression to down-regulate E-cadherin and enhance cell migration and invasion in colorectal cancer cells. *J Biol Chem*. 2013;288:9001–9010.
39. Braunstein M, Anderson MK. HEB in the spotlight: transcriptional regulation of T-cell specification, commitment, and developmental plasticity. *Clin Dev Immunol*. 2012;2012:678705.
40. Kugathasan S, Baldassano RN, Bradfield JP, Sleiman PM, Imielinski M, Guthery SL, Cucchiara S, Kim CE, Frackelton EC, Annaiah K, Glessner JT, Santa E, Willson T, Eckert AW, Bonkowski E, Shaner JL, Smith RM, Otieno FG, Peterson N, Abrams DJ, Chiavacci RM, Grundmeier R, Mamula P, Tomer G, Piccoli DA, Monos DS, Annese V, Denson LA, Grant SF, Hakonarson H. Loci on 20q13 and 21q22 are associated with pediatric-onset inflammatory bowel disease. *Nat Genet*. 2008;40:1211–1215.
41. UK IBD Genetics Consortium, Barrett JC, Lee JC, Lees CW, Prescott NJ, Anderson CA, Phillips A, Wesley E, Parnell K, Zhang H, Drummond H, Nimmo ER, Massey D, Blaszczyk K, Elliott T, Cotterill L, Dallal H, Lobo AJ, Mowat C, Sanderson JD, Jewell DP, Newman WG, Edwards C, Ahmad T, Mansfield JC, Satsangi J, Parkes M, Mathew CG, Wellcome Trust Case Control Consortium 2, Donnelly P, Peltonen L, Blackwell JM, Bramon E, Brown MA, Casas JP, Corvin A, Craddock N, Deloukas P, Duncanson A, Jankowski J, Markus HS, Mathew CG, McCarthy MI, Palmer CN, Plomin R, Rautanen A, Sawcer SJ, Samani N, Trembath RC, Viswanathan AC, Wood N, Spencer CC, Barrett JC, Bellenguez C, Davison D, Freeman C, Strange A, Donnelly P, Langford C, Hunt SE, Edkins S, Gwilliam R, Blackburn H, Bumpstead SJ, Dronov S, Gillman M, Gray E, Hammond N, Jayakumar A, McCann OT, Liddle J, Perez ML, Potter SC, Ravindrarajah R, Ricketts M, Waller M, Weston P, Widaa S, Whittaker P, Deloukas P, Peltonen L, Mathew CG, Blackwell JM, Brown MA, Corvin A, McCarthy MI, Spencer CC, Attwood AP, Stephens J, Sambrook J, Ouwehand WH, McArdle WL, Ring SM, Strachan DP. Genome-wide association study of ulcerative colitis identifies three new susceptibility loci, including the HNF4A region. *Nat Genet* 2009;41:1330–1334.
42. Sasaki T, Fassler R, Hohenester E. Laminin: the crux of basement membrane assembly. *J Cell Biol*. 2004;164:959–963.
43. Aszodi A, Legate KR, Nakchbandi I, Fassler R. What mouse mutants teach us about extracellular matrix function. *Annu Rev Cell Dev Biol*. 2006;22:591–621.
44. Jeanes A, Gottardi CJ, Yap AS. Cadherins and cancer: how does cadherin dysfunction promote tumor progression? *Oncogene*. 2008;27:6920–6929.
45. Bis JC, Kavousi M, Franceschini N, Isaacs A, Abecasis GR, Schminke U, Post WS, Smith AV, Cupples LA, Markus HS, Schmidt R, Huffman JE, Lehtimaki T, Baumert J, Munzel T, Heckbert SR, Dehghan A, North K, Oostra B, Bevan S, Stoegerer EM, Hayward C, Raitakari O, Meisinger C, Schillert A, Sanna S, Volzke H, Cheng YC, Thorsson B, Fox CS, Rice K, Rivadeneira F, Nambi V, Halperin E, Petrovic KE, Peltonen L, Wichmann HE, Schnabel RB, Dorr M, Parsa A, Aspelund T, Demissie S, Kathiresan S, Reilly MP, Taylor K,

Uitterlinden A, Couper DJ, Sitzer M, Kahonen M, Illig T, Wild PS, Orru M, Ludemann J, Shuldiner AR, Eiriksdottir G, White CC, Rotter JI, Hofman A, Seissler J, Zeller T, Usala G, Ernst F, Launer LJ, D'Agostino RB Sr, O'Leary DH, Ballantyne C, Thiery J, Ziegler A, Lakatta EG, Chilukoti RK, Harris TB, Wolf PA, Psaty BM, Polak JF, Li X, Rathmann W, Uda M, Boerwinkle E, Klopp N, Schmidt H, Wilson JF, Viikari J, Koenig W, Blankenberg S, Newman AB, Witteman J, Heiss G, Duijn C, Scuteri A, Homuth G, Mitchell BD, Gudnason V, O'Donnell CJ, CARDIoGRAM Consortium. Meta-analysis of genome-wide association studies from the CHARGE consortium identifies common variants associated with carotid intima media thickness and plaque. *Nat Genet*. 2011;43:940–947.

46. Franke A, McGovern DP, Barrett JC, Wang K, Radford-Smith GL, Ahmad T, Lees CW, Balschun T, Lee J, Roberts R, Anderson CA, Bis JC, Bumpstead S, Ellinghaus D, Festen EM, Georges M, Green T, Haritunians T, Jostins L, Latiano A, Mathew CG, Montgomery GW, Prescott NJ, Raychaudhuri S, Rotter JI, Schumm P, Sharma Y, Simms LA, Taylor KD, Whiteman D, Wijmenga C, Baldassano RN, Barclay M, Bayless TM, Brand S, Buning C, Cohen A, Colombel JF, Cottone M, Stronati L, Denson T, De Vos M, D'Inca R, Dubinsky M, Edwards C, Florin T, Franchimont D, Gearry R, Glas J, Van Gossum A, Guthery SL, Halfvarson J, Verspaget HW, Hugot JP, Karban A, Laukens D, Lawrance I, Lemann M, Levine A, Libioulle C, Louis E, Mowat C, Newman W, Panes J, Phillips A, Proctor DD, Regueiro M, Russell R, Rutgeerts P, Sanderson J, Sans M, Seibold F, Steinhart AH, Stokkers PC, Torkvist L, Kullak-Ublick G, Wilson D, Walters T, Targan SR, Brant SR, Rioux JD, D'Amato M, Weersma RK, Kugathasan S, Griffiths AM, Mansfield JC, Vermeire S, Duerr RH, Silverberg MS, Satsangi J, Schreiber S, Cho JH, Annese V, Hakonarson H, Daly MJ, Parkes M. Genome-wide meta-analysis increases to 71 the number of confirmed Crohn's disease susceptibility loci. *Nat Genet*. 2010;42:1118–1125.

47. Jostins L, Ripke S, Weersma RK, Duerr RH, McGovern DP, Hui KY, Lee JC, Schumm LP, Sharma Y, Anderson CA, Essers J, Mitrovic M, Ning K, Cleynen I, Theatre E, Spain SL, Raychaudhuri S, Goyette P, Wei Z, Abraham C, Achkar JP, Ahmad T, Amininejad L, Ananthakrishnan AN, Andersen V, Andrews JM, Baidoo L, Balschun T, Bampton PA, Bitton A, Boucher G, Brand S, Buning C, Cohain A, Cichon S, D'Amato M, De Jong D, Devaney KL, Dubinsky M, Edwards C, Ellinghaus D, Ferguson LR, Franchimont D, Fransen K, Gearry R, Georges M, Gieger C, Glas J, Haritunians T, Hart A, Hawkey C, Hedl M, Hu X, Karlsen TH, Kupcinskas L, Kugathasan S, Latiano A, Laukens D, Lawrance IC, Lees CW, Louis E, Mahy G, Mansfield J, Morgan AR, Mowat C, Newman W, Palmieri O, Ponsioen CY, Potocnik U, Prescott NJ, Regueiro M, Rotter JI, Russell RK, Sanderson JD, Sans M, Satsangi J, Schreiber S, Simms LA, Sventoraityte J, Targan SR, Taylor KD, Tremelling M, Verspaget HW, De Vos M, Wijmenga C, Wilson DC, Winkelmann J, Xavier RJ, Zeissig S, Zhang B, Zhang CK, Zhao H, International IBD Genetics Consortium (IIBDGC), Silverberg MS, Annese V, Hakonarson H, Brant SR, Radford-Smith G, Mathew CG, Rioux JD, Schadt EE, Daly MJ, Franke A, Parkes M, Vermeire S, Barrett JC, Cho JH. Host-microbe interactions have shaped the genetic architecture of inflammatory bowel disease. *Nature*. 2012;491:119–124.

48. Raines EW. PDGF and cardiovascular disease. *Cytokine Growth Factor Rev*. 2004;15:237–254.

49. Tang J, Kozaki K, Farr AG, Martin PJ, Lindahl P, Betsholtz C, Raines EW. The absence of platelet-derived growth factor-B in circulating cells promotes immune and inflammatory responses in atherosclerosis-prone ApoE-/- mice. *Am J Pathol*. 2005;167:901–912.

50. Kozaki K, Kaminski WE, Tang J, Hollenbach S, Lindahl P, Sullivan C, Yu JC, Abe K, Martin PJ, Ross R, Betsholtz C, Giese NA, Raines EW. Blockade of platelet-derived growth factor or its receptors transiently delays but does not prevent fibrous cap formation in ApoE null mice. *Am J Pathol*. 2002;161:1395–1407.

51. Wang X, Korstanje R, Higgins D, Paigen B. Haplotype analysis in multiple crosses to identify a QTL gene. *Genome Res*. 2004;14:1767–1772.

52. Lu Z, Yuan Z, Miyoshi T, Wang Q, Su Z, Chang CC, Shi W. Identification of Soat1 as a quantitative trait locus gene on mouse chromosome 1 contributing to hyperlipidemia. *PLoS ONE*. 2011;6:e25344.

53. Lorbek G, Lewinska M, Rozman D. Cytochrome P450s in the synthesis of cholesterol and bile acids–from mouse models to human diseases. *FEBS J*. 2012;279:1516–1533.

54. Rowlan JS, Zhang Z, Wang Q, Fang Y, Shi W. New quantitative trait loci for carotid atherosclerosis identified in an intercross derived from apolipoprotein E-deficient mouse strains. *Physiol Genomics*. 2013;45:332–342.